



HAL
open science

Contact pressure in the proton exchange membrane fuel cell: Development of analytical models based on experimental investigation and a posteriori design of experiments

Luca Marcelli, Dominique Chamoret, E. Mancini, X. François, Yann Meyer,
D. Candusso

► To cite this version:

Luca Marcelli, Dominique Chamoret, E. Mancini, X. François, Yann Meyer, et al.. Contact pressure in the proton exchange membrane fuel cell: Development of analytical models based on experimental investigation and a posteriori design of experiments. *Journal of Power Sources*, 2024, 617, pp.235158. 10.1016/j.jpowsour.2024.235158 . hal-04679114

HAL Id: hal-04679114

<https://cyu.hal.science/hal-04679114v1>

Submitted on 27 Aug 2024

HAL is a multi-disciplinary open access archive for the deposit and dissemination of scientific research documents, whether they are published or not. The documents may come from teaching and research institutions in France or abroad, or from public or private research centers.

L'archive ouverte pluridisciplinaire **HAL**, est destinée au dépôt et à la diffusion de documents scientifiques de niveau recherche, publiés ou non, émanant des établissements d'enseignement et de recherche français ou étrangers, des laboratoires publics ou privés.



Contact pressure in the proton exchange membrane fuel cell: Development of analytical models based on experimental investigation and a posteriori design of experiments

L. Marcelli^{a,b,c,d,e,*}, D. Chamoret^b, E. Mancini^a, X. François^d, Y. Meyer^c, D. Candusso^{d,e}

^a Università degli Studi dell'Aquila, Department of Industrial and Information Engineering and Economics, Piazzale Ernesto Pontieri, Monteluco di Roio, 67100, L'Aquila, Italy

^b ICB (UMR 6303), CNRS, Univ. Bourgogne Franche-Comté, UTBM, Belfort, France

^c Université Savoie Mont Blanc, SYMME, 74000, Annecy, France

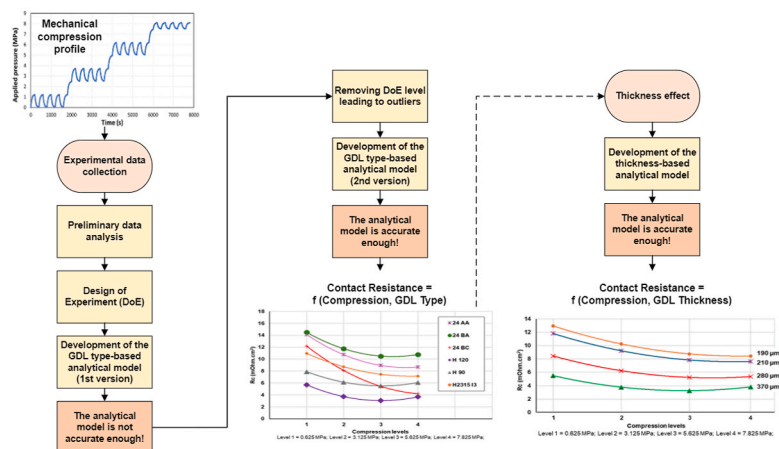
^d FCLAB, Plateforme Hydrogène Energie, UTBM, Rue Thierry Mieg, 90010, Belfort Cedex, France

^e SATIE (UMR CNRS 8029), Université Paris Saclay, ENS Paris Saclay, Université Gustave Eiffel, 25 Allée des Marronniers, 78000, Versailles Satory, France

HIGHLIGHTS

- The modelling is based on electrical Contact Resistance (CR) experimental results.
- Test results are classified to develop two models through a posteriori DoE approach.
- The first model reflects the benefit of MPL and the slight drawback of PTFE on CR.
- The 2nd model predicts that higher mechanical stress and thicker GDLs reduce CR.
- The modelling approach can be used for PEMFC design and component selection.

GRAPHICAL ABSTRACT



ARTICLE INFO

Keywords:

Fuel cell
Experimental design
Gas diffusion layer
Electrical contact resistance
Mechanical compression

ABSTRACT

To understand the link between the physical properties of the Gas Diffusion Layer (GDL) and the overall performance of a Proton Exchange Membrane Fuel Cell (PEMFC), it is essential to investigate the impact of compressive loading on the physical parameters of the component, focusing on its electrical properties. This paper's experimental results obtained in the team's previous research are classified and analysed using a posteriori Design of Experiment (DoE). It allows us to determine the influential parameters on the component behaviour. Two analytical models are developed through regression analysis, allowing for predicting the output

* Corresponding author. SATIE (UMR CNRS 8029), Université Paris Saclay, ENS Paris Saclay, Université Gustave Eiffel, 25 Allée des Marronniers, 78000, Versailles Satory, France

E-mail addresses: luca.marcelli@universite-paris-saclay.fr, luca.marcelli@utbm.fr (L. Marcelli).

<https://doi.org/10.1016/j.jpowsour.2024.235158>

Received 20 February 2024; Received in revised form 16 July 2024; Accepted 29 July 2024

Available online 5 August 2024

0378-7753/© 2024 The Authors. Published by Elsevier B.V. This is an open access article under the CC BY license (<http://creativecommons.org/licenses/by/4.0/>).

variables as a function of the input ones. The results are evaluated with statistical tools. The first model predicts the electrical Contact Resistance (CR) variation of the GDL as a function of mechanical compression and component type. The analytical results show that cycling compression has a negligible effect due to the lower number of applied cycles. The Micro Porous Layer (MPL) presence increases the CR, while the polytetrafluoroethylene (PTFE) decreases it slightly. The GDL thickness is the most influential geometrical parameter. For this reason, a second analytical model is developed and predicts that CR is reduced primarily by increased mechanical compression and thicker GDLs.

1. Introduction

Given the growing concern due to climate and environmental problems, the issue of energy use is one of the principal political and social debates of these times. A significant aspect of developing renewable energies is the possibility of efficiently converting solar, chemical, and thermal energy into electrical energy. In this regard, Fuel Cells (FCs) are closer than ever to meeting energy requirements as they can provide environmentally friendly energy conversion systems necessary for a world powered by renewable energies [1].

In the last decades, there has been a great interest in using low-temperature Proton Exchange Membrane Fuel Cells (PEMFCs) as an alternative to internal combustion engines and a promising technology for other applications [2]. They have advantages over other FCs for the relatively low working temperatures (from 50 to 120 °C), small volume and quick start. A PEMFC consists of different components, such as the End Plates (EPs), gaskets, BiPolar Plates (BPPs) and the Membrane Electrode Assembly (MEA), which in turn is composed of Catalyst Layers (CLs), Gas Diffusion Layers (GDLs) and a Proton Exchange Membrane (PEM) [3].

FCs are assembled by mechanical compression with fasteners (e.g., nuts and bolts). The assembly requires careful control to ensure optimal alignment of the different components and an appropriate assembly pressure to obtain optimal contacts between the elements (i.e., mechanical, thermal, and electrical) and ensure gas-tight operations. In addition to the assembly pressure, during the operation of the PEMFCs, various phenomena generate mechanical compression that can affect FC performance, such as the freeze/thaw cycles, the temperature and even the humidity. Indeed, FCs are systems where physical phenomena are coupled, and their interactions are very significant for the performance and durability of the technology.

Mechanical compression generates two main effects on a FC in service: the first is a positive effect, reducing the ohmic Contact Resistance (CR) between the various components; on the other hand, the second one is negative since it could increase the mass transportation resistance. For this reason, researchers are focusing on understanding the relationship between the electrical properties of PEMFC components and their variation under operating conditions [4]. In particular, GDL is the most impacted component. Its porous, fibrous structure and minimal thickness foster anisotropic, inhomogeneous, and non-linear physical properties. These lead to a non-linear stress-strain curve with a non-constant and anisotropic Young's modulus [5] and strain hysteresis, i.e. a sensitivity to the history of applied stresses [6–9].

Anisotropy of the compression modulus is observed between the in-plane direction (around 1–10 GPa [10]) and the through-plane direction (1–10 MPa in Ref. [10] and around 10–30 MPa in Ref. [8]). In the plane, the GDLs are also aligned in preferential directions (machine and cross-machine directions), where anisotropy is also observed [10].

Just as mechanical properties are affected by compression pressure, so are the electrical properties of GDLs. Two main electrical properties must be highlighted: contact and bulk resistance.

CR makes it difficult for electrical charges to pass through the contact surface between two bulk components. In fact, the actual contact area is smaller than it appears because contact surfaces are rough and uneven, which causes an increase in electrical resistance. This condition worsens in GDLs, made of porous fibre composite materials with an even smaller

contact area.

Determining a mean bulk resistivity (namely its through-plane and in-plane resistivity values) can be helpful since it is not easy to define all coefficients of the resistivity tensor. The through-plane resistivity is the resistance experienced by an electric current as it travels perpendicular to the GDL plane, from one side to the other. On the other hand, in-plane electrical resistivity refers to the resistance encountered by an electric current as it moves parallel to the plane of GDL. If GDLs are considered as isotropic, a commonly used method is to estimate the mean bulk resistivity through carbon-fibre and air ones and take into account the porosity ratio. The results showed that GDLs' electrical conductivity increases with compression while porosity decreases [11]. However, the direction dependence of the electrical resistance must be considered.

Because of the GDL structure, this conductivity/resistivity is anisotropic. In Ref. [12], researchers numerically estimated the through-plane and in-plane conductivities of carbon paper GDLs based on porosity. This analysis revealed that the in-plane conductivity exceeded the through-plane conductivity, aligning with experimentally determined conductivities across various levels of porosity induced by compression. M.S. Ismail et al. [13] were able to evaluate the effect of GDL anisotropy. They demonstrated that considering isotropic GDLs resulted in an over- or under-estimation of the average current density (23–30 %). Anisotropic GDLs showed a more uniform current density distribution and furthermore the in-plane anisotropy did not affect FC performance [14]. The through-plane resistance is higher than the in-plane one, which can be easily explained if we consider that electrons travel much more in GDL fibres that are all in the plane rather than going from one fibre to another located in the next plane. Both decrease with mechanical compression [15].

FCs can undergo hundreds of thousands of load cycles during their operational lifetime [16] and the effects of cyclic loading on the PEMFC performance are observed. In Ref. [6], it is demonstrated that the overall through-plane resistance of a GDL Sigracet® 24AA decreases as the number of loading and unloading cycles increases, with the most significant reduction occurring during the initial cycle, where it decreases by up to 50 %. Similarly, Sadeghifar et al. [17] present analogous findings, where cyclic loading and unloading lead to a decrease in the total resistance of a GDL Sigracet® 34BCE, with the most substantial reduction occurring during the first cycle, showing a decrease of approximately 30 %.

Considering the effect of the other operating conditions on GDL, Wen et al. [18] have analysed how different combinations of bolt configuration and clamping torque can affect the pressure distribution and overall performance of a single cell and a 10-cell PEMFC stack. Both the single-cell and the 10-cell stack showed better pressure distribution and maximum power density with increased clamping torque and the number of bolts. It is possible to explain this result by looking at the changes in the electrical CR and the GDL's porosity under mechanical compression because pressure uniformity reduces the ohmic resistance of the PEMFC, particularly the CR, consequently increasing the maximum power density.

Y. Faydi et al. [19] investigated the effects of dynamic mechanical loading on GDL compression modulus, which resulted in non-linear and insensitivity to the frequency of the dynamic excitation. Moreover, if static loads increase, the modulus increases, whereas the hysteresis effect decreases if the dynamic load increases. They also observed a linear

increase of the compression modulus alongside temperature up to 280 °C, after which it starts decreasing linearly.

PEMFC environment has high humidity and an increased temperature (60–90 °C). In Ref. [7], temperature had no significant effect on the stress-strain curve. But the humidity was found to soften GDL. Furthermore, polytetrafluorethylene (PTFE) was shown to affect and increase the rigidity of GDL.

Chen. Y [20] studied the compressive behaviour of GDLs, finding that it remains unchanged up to 60 °C. However, the compression resistance decreases at higher temperatures (90 °C). Chien C et al. [11] assembled a 12-bolt 3D-FEM model of PEMFC to predict the effect of compression on GDL and PEM performance. By conducting simulations involving a static load ranging from 1 to 7 MPa and a central thermal load, the researchers demonstrated that the maximum deformation of GDL occurs at the midpoint of BPP channel. This finding was consistent with the results obtained from a 2D model found in the literature [21]. Furthermore, the study revealed that the deformation caused by the smallest mechanical load is four times greater than that resulting from the thermal load.

In a separate investigation, Serincan M.F et al. [22] explored the influence of membrane water content on rigidity of GDL. They simulate three distinct GDL configurations with an isotropic membrane: a soft isotropic GDL, a rigid isotropic GDL, and an orthotropic GDL, which reflects a more realistic scenario with rigidity varying between in-plane and through-plane orientations. They then observed multiple water distribution scenarios, finding a difference in results when considering an isotropic GDL from real anisotropic properties of GDL. The soft GDL undergoes deformation, resulting in the same shape as the orthotropic GDL because the dimension ratios favour the through-plane direction. The study also reported a close GDL displacement shape between the through-plane water content variation and constant water content. Water distribution at the membrane-GDL interface remained consistent and stable in both scenarios.

Considering the impact of all the aforementioned operating conditions, experimental and numerical approaches were adopted by the team during the K. Bouziane's PhD work [4] to examine the effect of compression on the electrical properties of several structures of carbon paper GDLs. The experiments were principally focused on particular input parameters to identify their influence on one output parameter. An extensive test campaign was carried out, resulting in a wide available set

of experimental data. This paper aims to design a methodology approach to take advantage of these data through a posteriori Design of Experiment (DoE) methodology. After selecting the parameters, two analytical models are developed through regression analysis in order to predict the impact of the operating conditions on the electrical properties of the GDLs. The results are analysed through statistical tools to improve the models e.g. by removing the outliers.

This paper is organised as follows. The methodological framework of this study is described in Section 2. A brief description of the available experimental results is given in Section 3. In Section 4, the criteria for the parameters selection, the adopted statistical analysis and the results obtained by the developed analytical model are explained. The same procedure was used for the second model. It is described in Section 5, before the article's conclusions.

2. Methodological framework for analytical model development (Fig. 1)

2.1. Experimental data collection

The foundation of our analytical model development is based on the rigorous experimental data collection carried out by our research team (Fig. 1). Previous investigations into the electrical CR between the GDL and BPPs have yielded a substantial dataset. This latter encompasses various conditions including variations in mechanical compression, GDL types, and environmental conditions such as humidity and temperature [4].

2.2. Preliminary data analysis

Initial analyses of these experimental results entailed a classification and assessment to ascertain the quality and relevance of the data for modelling purposes. Through this preliminary scrutiny, we established the integrity and consistency of the data, paving the way for a robust DoE process.

2.3. Posteriori design of experiment

Employing a posteriori DoE, we meticulously structured the available data to identify the most influential parameters affecting GDL

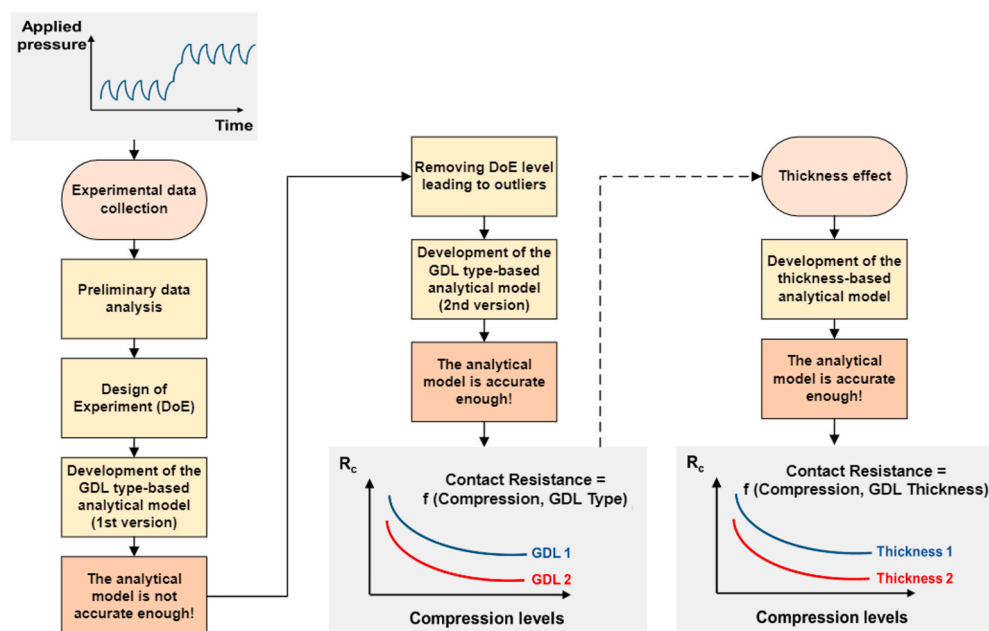


Fig. 1. Methodological framework for the analytical model development.

behaviour. The DoE approach facilitated a systematic exploration of the interactions between different variables and their collective impact on the electrical properties of the GDL.

2.4. Development of the GDL type-based analytical model (1st version)

The first version of our GDL type-based analytical model was derived from this stratified data. It sought to predict variations in CR as a function of mechanical compression, sensitivity of the cycling compression, and GDL type. Despite the model's initial promise, statistical evaluation suggested areas for improvement, particularly concerning the model's ability to accurately predict outcomes across all levels of mechanical compression.

2.5. Statistical evaluation of the GDL type-based analytical model (1st version)

We conducted a rigorous statistical assessment using analysis of variance (ANOVA) and regression analysis to refine the model. This statistical evaluation pinpointed inconsistencies and led to the removal of outlier data points that could skew the model's predictive accuracy.

2.6. Development of the GDL type-based analytical model (2nd version)

Subsequent to the removal of inconsistent data, we introduced the second version of the model. This revised model demonstrated improved accuracy in predicting the CR across different types of GDL under varying mechanical compression.

2.7. Statistical evaluation of the GDL type-based analytical model (2nd version)

The second version of the model underwent another round of statistical validation. The adjustments made in response to the initial evaluation solidified the model's reliability, as reflected in the more robust statistical parameters.

2.8. Results and interpretation of the GDL type-based analytical model

The outcomes of this iterative process confirmed the second version of the model as a reliable predictor of CR. The model adeptly accounted for the most influential factors, aligning closely with the empirical data.

2.9. Development of the thickness-based analytical model

To further the scope of our study, we developed a thickness-based analytical model. Recognising the paramount influence of GDL thickness on CR, this model was tailored to predict how variations in GDL thickness and mechanical compression affect CR.

2.10. Statistical evaluation of the thickness-based analytical model

The thickness-based model was also subjected to a thorough statistical evaluation, echoing the rigorous analytical approach employed throughout our study.

2.11. Results and interpretation of the thickness-based analytical model

The final iteration of our model effectively predicts CR trends based on GDL thickness, providing valuable insights for PEMFC design optimisation. It demonstrates the effectiveness of our methodological framework in leveraging experimental data for analytical model development.

3. Available experimental results

The carried out experimental campaign consists of three types of ex-situ experimentations to determine the electrical properties attributed to the ohmic losses in PEMFCs: electrical contact resistance (R_c), through-plane resistance (R_{tp}) and in-plane resistance (R_{ip}) [4]. Each investigation is focused on an electrical property of GDL. Furthermore, in order to study the effect of humidity, the through-plane resistance test was carried out with both dry and impregnated GDLs.

Different types of GDL have been deeply studied considering different physical properties, as well thickness, structural composition, presence of Micro Porous Layer (MPL) and PTFE. Moreover, the impacts of temperature, compression velocity, humidity and cyclic compression were also evaluated among the operating conditions.

Since the experimentations were thought individually, they do not have the same operating conditions, GDLs types and mechanical loading profiles. For this reason, a preliminary deep evaluation of the available results was done to avoid using parameters with missing information, e. g. developing a model with two different GDL samples investigated under different operating conditions. A summary of the investigated types of GDL and operating conditions in the various experiments are reported in [Tables 1 and 2](#), respectively.

By classifying the experimental results, it was possible to have a clear view of the available data and make the first evaluations for the project roadmap.

The DoE methodology was the adopted technique for structuring, presenting, and analysing the database in a rationally and robust way. The experiments plan is achieved by defining the inputs (the independent variables or factors), their levels (the interval of their variation) and the outputs, allowing to compute the variation of the outputs as a function of the inputs.

4. Development of a GDL type-based model

Since we intend to consider as many factors as possible among the available results, a methodological approach, defining a selection criterion for the parameters, was needed. The selection criterion aims to consider the highest number of comparable parameters from the available experimental results. For this reason, the operating conditions and the investigated GDL types were analysed in the three experimentations and then compared.

4.1. Parameters selection criterion

In the present study, the outputs are the electrical properties of GDL and the inputs the physical properties and the operating conditions that influence them.

The selection criterion consisted of analysing for each experiment.

- the number of GDL types investigated;
- the considered physical properties of the component;
- the applied operating conditions;
- the range of mechanical compression profiles;
- the number of applied mechanical cycles;
- the impact of the electrical properties on the ohmic losses.

As first evaluation we considered every carried-out experiment (one for each electrical property: contact, through-plane, and in-plane resistances). However, this approach presented some limitations.

- the range of the mechanical compression profiles is different for each experiment;
- some operating conditions, e.g. humidity, are not studied for each GDL sample;

Table 1
Investigated GDL and test types [4]. (R_c = Contact Resistance; R_{ip} = Through-plane Resistance; R_{ip} = In-plane resistance).

| GDL Types | Thickness (μm) | Structure | PTFE | MPL | R_c Test | R_{ip} Test | | R_{ip} Test |
|---------------------|-----------------------------|----------------------------|------|-----|------------|---------------|--------------------|---------------|
| | | | | | | Dry | Vapor impregnation | |
| SGL 24 AA | 190 | Carbonised straight fibre | No | No | x | x | x | x |
| SGL 24 BA | 190 | Carbonised straight fibre | Yes | No | x | x | x | x |
| SGL 24 BCE | 235 | Carbonised straight fibre | Yes | Yes | x | x | x | x |
| SGL 38 BCE | 325 | Carbonised straight fibre | Yes | Yes | | x | | x |
| SGL 35 AA | 300 | Carbonised straight fibre | No | No | | | x | |
| SGL 25 AA | 190 | Carbonised straight fibre | No | No | | | x | |
| SGL 10 BA | 400 | Felt structure | Yes | No | x | x | | x |
| Toray H120 | 370 | Graphitised straight fibre | No | No | x | x | x | x |
| Toray H60 | 190 | Graphitised straight fibre | No | No | | | x | |
| Toray H90 | 280 | Graphitised straight fibre | No | No | x | | | |
| Freudenberg H231513 | 210 | Felt structure | Yes | Yes | x | | | |
| Freudenberg H14C9 | 180 | Felt structure | Yes | Yes | | x | | x |

Table 2
Investigated operating conditions for each test type [4].

| | Cyclic Compression | Temperature | Humidity | Compression velocity |
|---------------|--------------------|-------------|----------|----------------------|
| R_c Test | x | x | | x |
| R_{ip} Test | x | x | x | |
| R_{ip} Test | x | | x | |

- only four GDL types are investigated in all the experiments (SGL 24 AA, SGL 24 BA, SGL 24 BCE and H120). So, a restricted number of physical properties was considered.

Subsequently we decided of considering the single experiment [4,23] and trying to obtain significant results for the ohmic losses. The following considerations were done.

- the electrical CR between GDL and BPP is one of the major causes of ohmic losses in PEMFC and, therefore, is of greater importance for FC performance [10,24];

- the mechanical compression profile applied to GDLs in the first experiment (see Fig. 2a) has a larger compression range and a higher number of cycles. It allows to consider the effect of cyclic compression;
- the number of GDLs studied in the first experiment is high enough to consider different characteristics, including thickness, structural composition, PTFE presence, and MPL coating.

By the first investigation, enough data to select the parameters necessary to develop the analytical model were obtained. The chosen inputs, with the respective levels, are reported in Table 3.

The choice of GDL as first parameter is related to the opportunities of evaluating the effects of the different physical characteristics of the layer. The results relating to six types of GDL, with the SGL 24 BCE investigated in both MPL and Porous Transport Layer (PTL) sides, are available. By these seven levels, it has been possible to analyse different thicknesses, three types of structural composition, the presence of PTFE, and the MPL coating.

The second factor chosen is the *mechanical compression*. It is characterised by four small ranges in which the element is subjected to compression cycles (see Fig. 2a). Therefore, the number of levels chosen is four, one for each range of repeated cycles. It was considered appropriate to choose the mean value of the cycle, the latter identified by the ascent and descent peak (see Fig. 2b).

The *cycle number* was chosen as a third factor. The cycles accepted are from the second to the fifth, whereas the first one was discarded due to the settling of the test. For the choice of the levels of this factor, both the rising and falling values of the mechanical compression cycle were taken into account, to consider the hysteresis effect (see Fig. 2b).

4.2. Statistical evaluation of the results

Once the number of DoE factors and their level have been set, it is possible to calculate how many observations could be necessary to study the influence of the factors taken into consideration.

$$N = n \times L^F = 3 \times (7^2 \times 4^1) = 3 \times 196 \text{ observations} \tag{1}$$

Where N , n , L and F are the number of observations (number of total experiments), the number of repetitions, the number of levels, and the number of factors respectively.

As already mentioned, for each observation of the experimentation, three tests were performed. For the development of the model, the average of the obtained values has been used.

The analytical model was developed through a multilinear regression analysis and the results were evaluated by the ANOVA. It is a statistical method used to compare the means of three or more groups to determine if there are significant differences between them. The ANOVA method calculates the F-statistic, which is the ratio of the variance between the group means to the variance within the groups. The p-value is then used

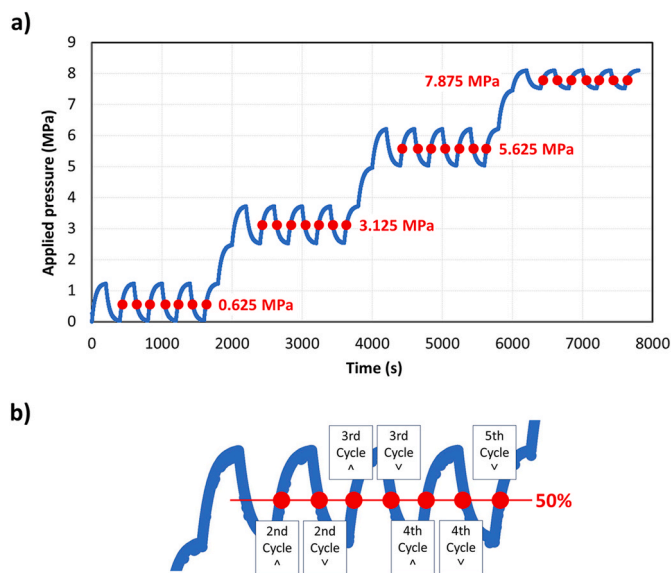


Fig. 2. a) Compression cycles and the mean value for each of them; b) Choice of values in the generic range of the mechanical compression profile applied to the GDL.
(\blacktriangle : Mechanical compression ascent. \blacktriangledown : Mechanical compression descent).

Table 3Factors and levels of the first DoE (\wedge : Mechanical compression ascent. \vee : Mechanical compression descent).

| Factors | Level 1 | Level 2 | Level 3 | Level 4 | Level 5 | Level 6 | Level 7 |
|--|--------------------|--------------------|--------------------|--------------------|-------------------|------------------|------------------|
| A GDL types | 24 AA | 24 BA | 24 BCE (MPL side) | H 120 | 24 BCE (PTL side) | H 90 | H2315 I3 |
| B Compression (MPa) | 0.625 | 3.125 | 5.625 | 7.875 | | | |
| C Sensitivity to cycles compression | 2nd cycle \wedge | 3rd cycle \wedge | 4th cycle \wedge | 5th cycle \wedge | 2nd cycle \vee | 3rd cycle \vee | 4th cycle \vee |

to assess the significance of the F-statistic; if the p-value is below a specified threshold (usually 0.05), it suggests that at least one group mean is significantly different from the others [25].

Since adding a variable to the regression model causes the sum of squares to increase and the error sum of squares to decrease, the analyses were carried out iteratively to identify the less influential interactions preliminarily to remove them. Deciding whether the increase in the regression sum of squares is sufficient to warrant using an additional variable in the model has been fundamental. Adding an unimportant variable can increase the mean square error, thereby decreasing the model's usefulness [26]. Employing diagnostic tools such as the Shapiro-Wilk and D'Agostino-Pearson tests [27,28] enabled us to ascertain that the model's population does not adhere to a normal distribution. This latter is a significant condition for the model's reliability. Furthermore, the use of influence diagrams, including the Externally Studentised Residual Plot, DFFITS, and Cook's Distance, revealed that certain observations are marked by significantly high error values, identifying them as outliers within the model [25]. For the sake of conciseness, only the Externally Studentised Residual Plot is illustrated in this article (refer to Fig. 3a).

These outliers are specifically associated with observations that involve the PTL side of GDL 24 BCE, corresponding to the 5th level of factor A (e.g., 5th, 12th, 19th observations, etc.). As previously mentioned, our analysis encompasses both sides of GDL 24 BCE to account for the unique presence of the MPL coating on one side only.

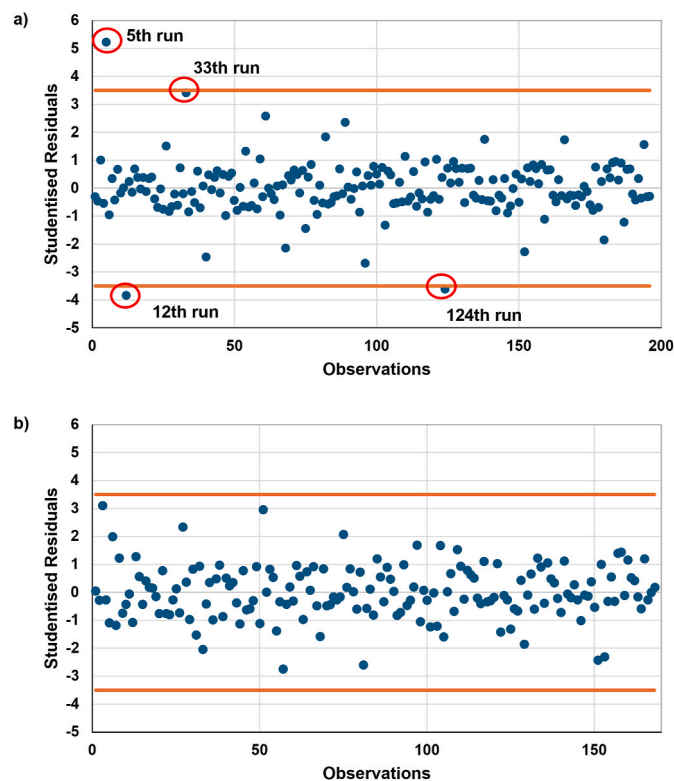


Fig. 3. Externally Studentised Residuals Plot: a) for the 1st version of the model (with 7 levels for the 1st factor). b) for the 2nd version of the model (with 6 levels for the 1st factor).

While the MPL reduces the CR between GDL and BPP, since the contact surface between the two elements increases, the PTL side greatly increases it. Considering this latter in the present model leads to very high errors, and the model reliability suffers. For this reason, having a normal distribution along a straight line is impossible. Moreover, such high CR values are not comparable with other GDLs and confirm that they do not provide helpful information for the present study.

With the evaluations made, it was considered appropriate to eliminate the PTL side of the 24BCE GDL type from the DoE and study a modified and improved model. The new inputs, with the respective levels, are reported in Table 4.

Since a level was eliminated for the first factor, it was necessary to recalculate the number of observations needed.

$$N = n \times L^f = 3 \times (6^1 \times 4^1 \times 7^1) = 3 \times 168 \text{ observations} \quad (2)$$

Before building the definitive model, preliminary ANOVA analyses were performed to select the most influential interactions. In Table 5 is shown the Full Factorial Design of the developed DoE.

The statistical tools mentioned before made it possible to confirm that the model's population is normally distributed, and the outliers are eliminated, assuring that all the assumptions required to verify the reliability of the model are respected (see Fig. 3b and Table 6).

4.3. Results

Once the reliability of the model is confirmed, evaluating the obtained analytical model is possible.

By the multiple linear regression, the analytical model of the output as a function of the inputs was obtained. It is the sum of the intercept and product of the factors and the respective coefficients.

$$\begin{aligned} R_c = & 103.32 - 183.93A - 41.77B + 141.51A^2 + 0.79B^2 + 75.36AB \\ & - 54.47A^2B - 0.01A^2B^2 - 48.76A^3 + 17.63A^3B + 7.6A^4 - 2.61A^4B \\ & - 0.44A^5 + 0.14A^5B \end{aligned} \quad (3)$$

With this model, it is possible to represent in a single graph the values obtained analytically (predicted values) and the experimental values obtained in Refs. [4,23].

Fig. 4 shows the CR values as a function of the levels chosen for the sensitivity to cycles compression (the C factor). The experimental results of all levels of the first factor (types of GDL) were averaged. This plot confirms the little influence that the shape of the applied mechanical compression profile cycles has on the CR variation. This neglectable effect is due to the lack of consideration of the first cycle of the applied mechanical profile. Without it, the effect of the other cycles on the electrical CR is negligible.

In Fig. 5a are shown the experimental and analytical results of the CR as a function of mechanical compression variation for each GDL. The experimental error bars are related to the GDL effect. By its analysis it is possible to confirm that the results of the analytical model approximate the experimental data quite well with respect to the uncertainties. Whereas, in Fig. 5b are reported the predicted CR results as a function of the applied compression for each GDL type.

This analytical model represents the first step for further models that can be extended by adding parameters, operating conditions and GDL types. For example, by observing the results obtained and knowing the characteristics of the different GDLs, it is possible to make some initial

Table 4
Factors and levels of the improved DoE (^: Mechanical compression ascent. v: Mechanical compression descent).

| Factors | Level 1 | Level 2 | Level 3 | Level 4 | Level 5 | Level 6 | Level 7 | |
|---------|-----------------------------------|-------------|-------------|--------------|-------------|-------------|-------------|-------------|
| A | GDL types | 24 AA | 24 BA | 24 BCE (MPL) | H 120 | H 90 | H2315 I3 | |
| B | Compression (MPa) | 0.625 | 3.125 | 5.625 | 7.875 | | | |
| C | Sensitivity of cycles compression | 2nd cycle ^ | 3rd cycle ^ | 4th cycle ^ | 5th cycle ^ | 2nd cycle v | 3rd cycle v | 4th cycle v |

Table 5
Full factorial design DoE.

| Runs | Factors | | | | | | | | | | | | | | | Output |
|------|--|---|---|----------------|----------------|----------------|----|------------------|-------------------------------|----------------|------------------|----------------|------------------|----------------|------------------|--|
| | A | B | C | A ² | B ² | C ² | AB | A ² B | A ² B ² | A ³ | A ³ B | A ⁴ | A ⁴ B | A ⁵ | A ⁵ B | Contact Resistance |
| 1 | 3 Factors | | | | | | | | | | | | | | | 3 Repetitions: Y ₁ , Y ₂ , Y ₃ , Y _{average} |
| 2 | 12 Interactions | | | | | | | | | | | | | | | |
| 3 | 168 x 3 Observations (Total number of Experiments) | | | | | | | | | | | | | | | |
| ... | | | | | | | | | | | | | | | | |
| ... | | | | | | | | | | | | | | | | |
| 168 | | | | | | | | | | | | | | | | |

Table 6
ANOVA, Shapiro-Wilk Test, and d'Agostino-Pearson Test results.
A = GDL type; B = Compression; C = Sensitivity to the cyclic compression.

| ANOVA | Degrees of Freedom | Sum of Squares | Mean of Squares | Alpha F-statistic | 0.05 p-value | Significant |
|------------|--------------------|----------------|-----------------|----------------------|-----------------|-------------|
| Regression | 15 | 1717.67 | 114.51 | 322.39 | 6.03E-107 | Yes |
| Residual | 152 | 53.99 | 0.36 | | | |
| Total | 167 | 1771.66 | | | | |

| | Coefficients | Standard Error | t-statistic | p-value |
|-------------------------------|--------------|----------------|-------------|-----------|
| Intercept | 103.323 | 8.392 | 12.313 | 1.329E-24 |
| A | -183.93 | 17.448 | -10.542 | 7.603E-20 |
| B | -41.769 | 3.082 | -13.551 | 6.232E-28 |
| C | -0.066 | 0.109 | -0.608 | 0.5443829 |
| A ² | 141.512 | 12.729 | 11.117 | 2.188E-21 |
| B ² | 0.788 | 0.073 | 10.746 | 2.168E-20 |
| C ² | 0.001 | 0.013 | 0.050 | 0.9602220 |
| A.B | 75.365 | 6.371 | 11.829 | 2.667E-23 |
| A ² B | -54.474 | 4.648 | -11.720 | 5.247E-23 |
| A ² B ² | -0.008 | 0.004 | -2.219 | 0.0279768 |
| A ³ | -48.766 | 4.199 | -11.615 | 1.007E-22 |
| A ³ B | 17.634 | 1.533 | 11.502 | 2.027E-22 |
| A ⁴ | 7.601 | 0.639 | 11.887 | 1.858E-23 |
| A ⁴ B | -2.610 | 0.233 | -11.180 | 1.488E-21 |
| A ⁵ | -0.437 | 0.036 | -11.970 | 1.112E-23 |
| A ⁵ B | 0.144 | 0.013 | 10.817 | 1.395E-20 |

| Shapiro-Wilk Test | | d'Agostino-Pearson Test | |
|-------------------|----------|-------------------------|----------|
| W-stat | 0.985214 | DA-stat | 4.798215 |
| p-value | 0.072218 | p-value | 0.090798 |
| alpha | 0.05 | alpha | 0.05 |
| normal | Yes | normal | Yes |

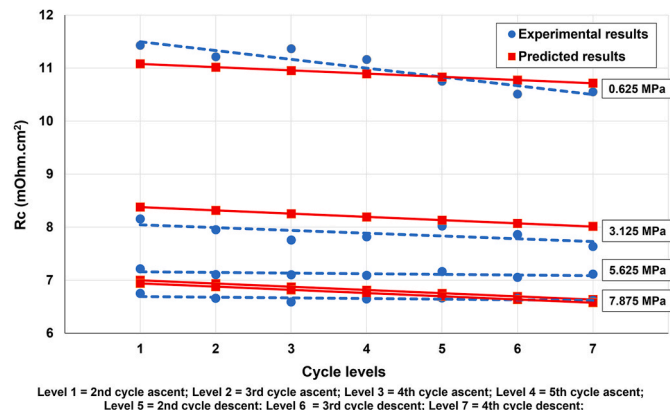


Fig. 4. R_c as a function of the cycles of the applied mechanical compression.

conclusions and confirm some results obtained in Refs. [4,23].

First, evaluating the results obtained for the first two types of GDL (24 AA and 24 BA), by considering that their only difference is the presence of PTFE, it is possible to confirm that it increases the CR. The presence of MPL coating reduces the CR since it increases the contact surface that is present between GDL and BPP. Furthermore, as mechanical compression increases, this phenomenon is more pronounced than in other GDLs. Secondly, for what concerns the thickness of GDL, it represents the physical property that most influences the decrease of the CR. As shown in Figs. 5b and 6, the thickness variation has a more significant influence on the CR (see the difference between 24 AA, 190 μm and H120, 380 μm) than the different structural compositions (increasing mechanical compression, the CR decreases equally for all the GDL except for the 24 BCE that has the MPL coating). This thickness effect is highlighted also in Ref. [29]. Consequently, it was considered appropriate to develop a smaller DoE to obtain an analytical model to

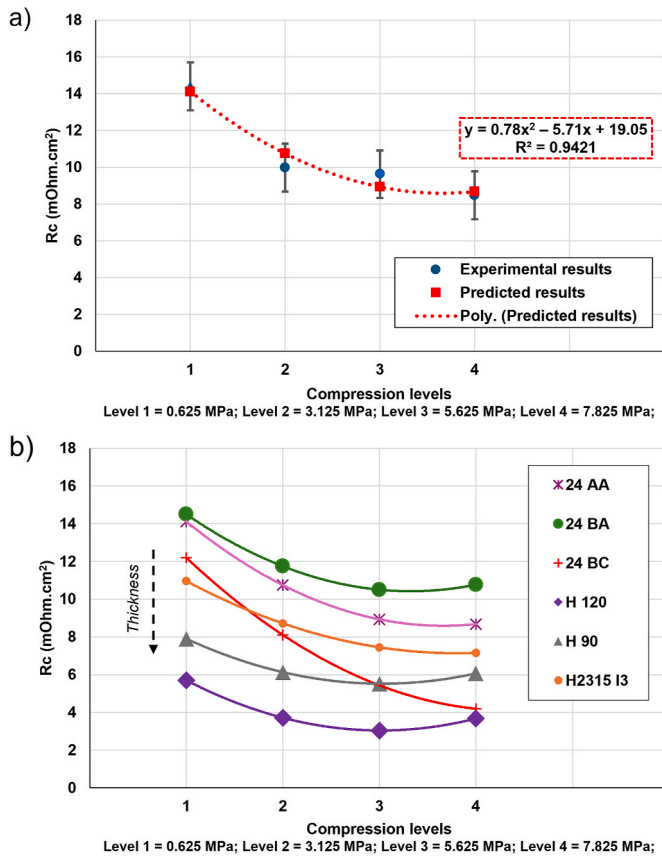


Fig. 5. a) Experimental and predicted results comparison. GDL type: SGL 24 AA. b) Predicted results for each GDL types.

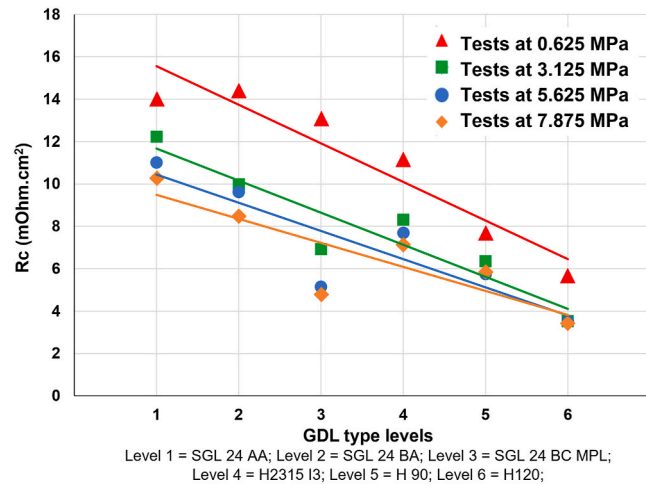


Fig. 6. R_c as a function of the type of GDL for each mechanical compression level.

predict the change in CR as a function of the thickness of GDL and the mechanical compression applied.

5. Development of a GDL thickness-based model

5.1. Parameters selection criterion

The thickness and the applied mechanical compression have been selected as the factors in the second model. Four levels have been chosen

Table 7

Factors and levels chosen for the second DoE.

| Factors | | Level 1 | Level 2 | Level 3 | Level 4 |
|---------|-------------------|---------|---------|---------|---------|
| A | Thickness (μm) | 190 | 210 | 280 | 370 |
| B | Compression (MPa) | 0.625 | 3.125 | 5.625 | 7.875 |

for the factor *thickness*. The thickness of 24 BCE was not considered in this model since the presence of the MPL, as shown, affects the CR in a completely different way. Among the GDL investigated, 24 AA and 24 BA have a thickness of 190 μm. For the development of this DoE, only one was adopted. Precisely, the experimental results obtained with the investigation of the SGL 24 AA were used. The same levels of the previous DoE were chosen for the *mechanical compression* factor. Moreover, since, in this case, we neglected the factor sensitivity to compression cycles, to use comparable experimental data, those relating to the fifth cycle of the generic range of the applied compression profile have been chosen.

The factors and the levels chosen are given in Table 7.

5.2. Statistical evaluation of the results

As with the other models, ANOVA analysis and multi-linear regression were performed to create the analytical model. The coefficients of multiple determination R² and R_{adj}² having high values (>0.97) confirm the model significance.

5.3. Results

With the ANOVA analysis, it was possible to define the significance of the interactions and create the following analytical model.

$$R_c = 28.62 - 0.09 \times A - 1.84 \times B + 0.09 \times B^2 + 0.002 \times A \times B \quad (4)$$

Fig. 7 shows predicted results of the obtained model for each thickness level. Whereas, the response surface plot of the CR results as a function of the thickness and mechanical compression is shown in Fig. 8.

Based on the obtained results it can be affirm that the model created can be used to predict the CR trend as a function of the thickness of GDL, even if it foresees a different structural composition or the presence of PTFE, since they have a smaller influence than the GDL thickness. On the other hand, if MPL coating is foreseen since it greatly influences this electrical property, the model is unsuitable for predicting reliable data. In the future, with further investigations, it will be possible to expand the model by considering other operating conditions as well.

6. Conclusions

The main objective of this paper was to create an analytical model that allows predicting the influence of various factors, on the electrical

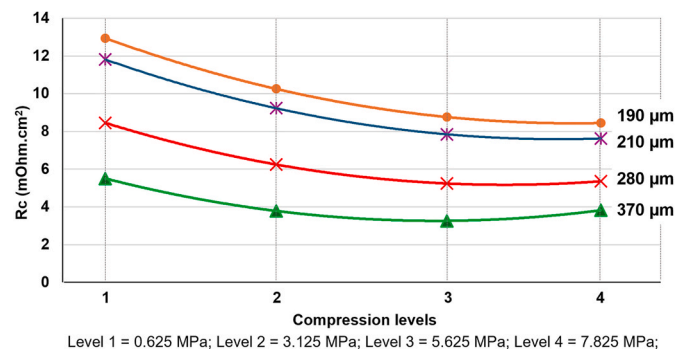


Fig. 7. – R_c as a function of the mechanical compression for each thickness level.

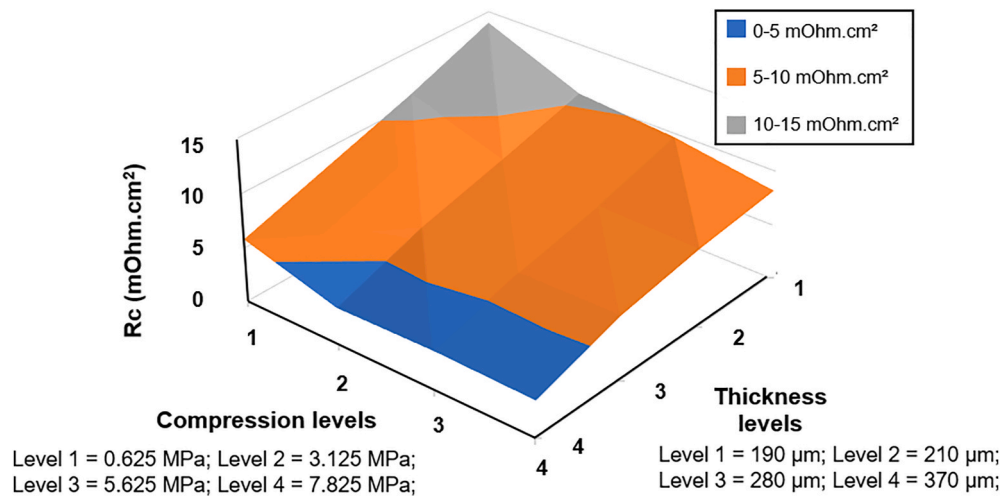


Fig. 8. Response surface plot: R_c as a function of the mechanical compression and thickness variation.

properties of the GDL during the PEMFC operation.

By employing a posteriori Design of Experiments (DoE) approach, we classified the experimental data obtained by the research team during K. Bouziane's PhD thesis work and developed a comprehensive model through regression analysis and ANOVA.

Two DoE were implemented. The first DoE was discarded as it was deemed unreliable. An improved model was created by eliminating both factors (e.g. compression cycles) and GDL levels (e.g. the GDL 24 BCE PTL side). Multiple linear regression was performed to obtain the analytical model. It allowed us to predict the CR variation as a function of the chosen factors.

Through the analytical model, it is possible to confirm some of the results obtained experimentally and to make the following considerations. The first two GDL types, 24 AA and 24 BA, are differentiated solely by the presence of PTFE. The inclusion of PTFE in 24 BA marginally elevates the CR. In contrast, the addition of a MPL coating leads to a reduction in CR, attributable to the enlarged contact interface between the GDL and BPP. Notably, this reduction in CR is more pronounced with increased mechanical compression, a trend that is distinctly more evident in these GDL types compared to others.

The thickness of GDL has a higher influence than the other physical characteristics. For this reason, a two-factor DoE that considered thickness and mechanical compression for studying the variation in CR was developed. This last version made it possible to confirm that higher values of mechanical compression (5.625 MPa and 7.875 MPa) and thicker GDLs, such as H90 and H120 (280 μm and 370 μm , respectively), result in lower CR.

The proposed analytical modelling approach allows studying the effect of mechanical compression on PEMFCs, which could be ideal for future FC design to improve their performance. Further investigations would allow to obtain experimental results to expand and create models with additional operating conditions and influencing parameters. Finally, other analytical models can be created to study the in-plane and through-plane resistances of GDL and the electrical properties of the other PEMFC components.

CRedit authorship contribution statement

L. Marcelli: Writing – original draft, Validation, Software, Methodology, Investigation, Formal analysis, Data curation, Conceptualization. **D. Chamoret:** Writing – review & editing, Validation, Supervision, Resources, Project administration, Methodology, Funding acquisition, Formal analysis, Data curation, Conceptualization. **E. Mancini:** Writing – review & editing, Validation, Supervision, Project administration, Methodology, Funding acquisition, Formal analysis, Data curation,

Conceptualization. **X. François:** Writing – review & editing, Validation, Supervision, Project administration, Methodology, Formal analysis, Data curation, Conceptualization. **Y. Meyer:** Writing – review & editing, Validation, Supervision, Project administration, Methodology, Funding acquisition, Data curation, Conceptualization. **D. Candusso:** Writing – review & editing, Validation, Supervision, Project administration, Methodology, Funding acquisition, Formal analysis, Data curation, Conceptualization.

Declaration of competing interest

The authors declare that they have no known competing financial interests or personal relationships that could have appeared to influence the work reported in this paper.

Data availability

Data will be made available on request.

Acknowledgements

L.M. received financial support for this project while he was affiliated at Università degli Studi dell'Aquila, Université Savoie Mont Blanc, ICB (UMR 6303), FCLAB - Plateforme Hydrogène Energie - UTBM.

References

- [1] T.V.D. Roches, M. Omiya, Failure prediction for membrane Electrode assembly, *J. Comput. Sci. Technol.* 7 (2) (2013) 221–230, <https://doi.org/10.1299/jcst.7.221>.
- [2] E.M. Khetabi, Behavioural analysis of PEM fuel cell components and research of causal relationships between in-situ and ex-situ observed performances [Online]. Available: <http://www.theses.fr/2021UPAST044/document>, 2021.
- [3] E.M. Khetabi, K. Bouziane, N. Zamel, X. Francois, Y. Meyer, D. Candusso, Effects of mechanical compression on the performance of polymer electrolyte fuel cells and analysis through in-situ characterisation techniques - a review, *J. Power Sources* 424 (Jun. 2019) 8–26, <https://doi.org/10.1016/j.jpowsour.2019.03.071>.
- [4] K. Bouziane, Study of the relations between the performances of PEM fuel cell components and their behaviors in stacks operated in the complete system. Development of Electrical and Mechanical Characterization Techniques, 2021 [Online]. Available: <http://www.theses.fr/2021UPAST066/document>.
- [5] J. Kleemann, F. Finsterwalder, W. Tillmetz, Characterisation of mechanical behaviour and coupled electrical properties of polymer electrolyte membrane fuel cell gas diffusion layers, *Sel. Pap. Present. 11th ULM Electrochem. Days* 190 (1) (May 2009) 92–102, <https://doi.org/10.1016/j.jpowsour.2008.09.026>.
- [6] H. Sadeghifar, In-plane and through-plane electrical conductivities and contact resistances of a Mercedes-Benz catalyst-coated membrane, gas diffusion and micro-porous layers and a Ballard graphite bipolar plate: impact of humidity, compressive load and polytetrafluoroethylene, *Energy Convers. Manag.* 154 (Dec. 2017) 191–202, <https://doi.org/10.1016/j.enconman.2017.10.060>.

- [7] S. Roohparvarzadeh, Experimental characterization of the compressive behaviour of gas diffusion layers in PEM fuel cells, UWSpace (2014) [Online]. Available: <http://hdl.handle.net/10012/8906>.
- [8] V. Norouzfard, M. Bahrami, Deformation of PEM fuel cell gas diffusion layers under compressive loading: an analytical approach, *J. Power Sources* 264 (Oct. 2014) 92–99, <https://doi.org/10.1016/j.jpowsour.2014.04.057>.
- [9] P.A. Gigos, Y. Faydi, Y. Meyer, Mechanical characterization and analytical modeling of gas diffusion layers under cyclic compression, *Int. J. Hydrogen Energy* 40 (17) (May 2015) 5958–5965, <https://doi.org/10.1016/j.ijhydene.2015.02.136>.
- [10] V. Mishra, F. Yang, R. Pitchumani, Measurement and prediction of electrical contact resistance between gas diffusion layers and bipolar plate for applications to PEM fuel cells, *J. Fuel Cell Sci. Technol.* 1 (1) (Mar. 2004) 2–9, <https://doi.org/10.1115/1.1782917>.
- [11] C.-H. Chien, et al., Effects of bolt pre-loading variations on performance of GDL in a bolted PEMFC by 3-D FEM analysis, *Energy* 113 (Oct. 2016) 1174–1187, <https://doi.org/10.1016/j.energy.2016.07.075>.
- [12] N. Zamel, X. Li, J. Shen, Numerical estimation of the effective electrical conductivity in carbon paper diffusion media, 1 Green Energy 2Special Sect. Pap. Present. 2nd Int. Energy 2030 Conf 93 (May 2012) 39–44, <https://doi.org/10.1016/j.apenergy.2011.08.037>.
- [13] M.S. Ismail, K.J. Hughes, D.B. Ingham, L. Ma, M. Pourkashanian, Effects of anisotropic permeability and electrical conductivity of gas diffusion layers on the performance of proton exchange membrane fuel cells, *Appl. Energy* 95 (Jul. 2012) 50–63, <https://doi.org/10.1016/j.apenergy.2012.02.003>.
- [14] M.S. Ismail, T. Damjanovic, D.B. Ingham, M. Pourkashanian, A. Westwood, Effect of polytetrafluoroethylene-treatment and microporous layer-coating on the electrical conductivity of gas diffusion layers used in proton exchange membrane fuel cells, *J. Power Sources* 195 (9) (May 2010) 2700–2708, <https://doi.org/10.1016/j.jpowsour.2009.11.069>.
- [15] A. Miyazawa, T. Himeno, A. Nishikata, Electrical properties of bipolar plate and gas diffusion layer in PEFC, *J. Power Sources* 220 (Dec. 2012) 199–204, <https://doi.org/10.1016/j.jpowsour.2012.07.127>.
- [16] M.K. Debe, Electrocatalyst approaches and challenges for automotive fuel cells, *Nature* 486 (7401) (Jun. 2012) 43–51, <https://doi.org/10.1038/nature11115>.
- [17] H. Sadeghifar, N. Djilali, M. Bahrami, Effect of Polytetrafluoroethylene (PTFE) and micro porous layer (MPL) on thermal conductivity of fuel cell gas diffusion layers: modeling and experiments, *J. Power Sources* 248 (Feb. 2014) 632–641, <https://doi.org/10.1016/j.jpowsour.2013.09.136>.
- [18] C.-Y. Wen, Y.-S. Lin, C.-H. Lu, Experimental study of clamping effects on the performances of a single proton exchange membrane fuel cell and a 10-cell stack, *J. Power Sources* 192 (2) (Jul. 2009) 475–485, <https://doi.org/10.1016/j.jpowsour.2009.03.058>.
- [19] Y. Paydi, R. Lachat, Y. Meyer, Thermomechanical characterisation of commercial gas diffusion layers of a proton exchange membrane fuel cell for high compressive pre-loads under dynamic excitation, *Fuel* 182 (Oct. 2016) 124–130, <https://doi.org/10.1016/j.fuel.2016.05.074>.
- [20] Y. Chen, C. Jiang, C. Cho, An investigation of the compressive behavior of polymer Electrode membrane fuel cell's gas diffusion layers under different temperatures, *Polymers* 10 (9) (2018), <https://doi.org/10.3390/polym10090971>.
- [21] P. Zhou, C.W. Wu, G.J. Ma, Contact resistance prediction and structure optimization of bipolar plates, *J. Power Sources* 159 (2) (Sep. 2006) 1115–1122, <https://doi.org/10.1016/j.jpowsour.2005.12.080>.
- [22] M.F. Serincan, U. Pasaogullari, Effect of gas diffusion layer anisotropy on mechanical stresses in a polymer electrolyte membrane, *J. Power Sources* 196 (3) (Feb. 2011) 1314–1320, <https://doi.org/10.1016/j.jpowsour.2010.06.026>.
- [23] K. Bouziane, E.M. Khetabi, R. Lachat, N. Zamel, Y. Meyer, D. Candusso, Impact of cyclic mechanical compression on the electrical contact resistance between the gas diffusion layer and the bipolar plate of a polymer electrolyte membrane fuel cell, *Renew. Energy* 153 (Jun. 2020) 349–361, <https://doi.org/10.1016/j.renene.2020.02.033>.
- [24] Y. Hou, B. Zhou, W. Zhou, C. Shen, Y. He, An investigation of characteristic parameter variations of the polarization curve of a proton exchange membrane fuel cell stack under strengthened road vibrating conditions, *Int. J. Hydrogen Energy* 37 (16) (Aug. 2012) 11887–11893, <https://doi.org/10.1016/j.ijhydene.2012.05.030>.
- [25] D.C. Howell, Statistical methods for psychology, in: Business Statistics Series, Duxbury Press, 1997 [Online]. Available: <https://books.google.it/books?id=ktkkAQAIAAJ>.
- [26] D.C. Montgomery, Design and Analysis of Experiments, second ed., Wiley, New York, 1984. ©1984, 1984. [Online]. Available: <https://search.library.wisc.edu/catalog/999529863402121>.
- [27] S.S. Shapiro, M.B. Wilk, An analysis of variance test for normality (complete samples), *Biometrika* 52 (3–4) (Dec. 1965) 591–611, <https://doi.org/10.1093/biomet/52.3-4.591>.
- [28] R. D'Agostino, E.S. Pearson, Tests for departure from normality. Empirical results for the distributions of b_2 and $\sqrt{b_1}$, *Biometrika* 60 (3) (1973) 613–622, <https://doi.org/10.2307/2335012>.
- [29] S. El Oualid, R. Lachat, D. Candusso, Y. Meyer, Characterization process to measure the electrical contact resistance of Gas Diffusion Layers under mechanical static compressive loads, Spec. Issue 1st Int. Conf. Adv. Energy Mater. AEM2016 12-14 Sept. 2016 Surrey Engl 42 (37) (Sep. 2017) 23920–23931, <https://doi.org/10.1016/j.ijhydene.2017.03.130>.